

Contents lists available at Dergipark

Journal of Scientific Reports-A

journal homepage: https://dergipark.org.tr/tr/pub/jsr-a



E-ISSN: 2687-6167 Number 62, September 2025

RESEARCH ARTICLE

Receive Date: 06.07.2025 Accepted Date: 11.09.2025

Investigation of physicochemical and filtration performances of Agdoped PVDF-cellulose composites prepared by different precipitation methods

Huseyin Gumus^{a,*}

^{a,*}Bilecik Seyh Edebali University, Osmaneli Vocational School, 11500, Osmaneli, Bilecik/Türkiye, ORCID: 0000-0002-2029-7978

Abstract

In this study, the physical and filtration properties of PVDF-Cellulose polymeric composites containing silver particles were prepared with two different methods and their structure were investigated. In the first method, precipitation with NaBH $_4$ in solution medium (method I), and in the second method, composites were prepared according to phase separation by mixing previously precipitated powder. The molecular interactions of the prepared samples were analysed by FTIR spectroscopy, and the surface properties were imaged by SEM device. Changes in the thermal resistance of the composites were investigated by TG-DTA analysis. Filtration properties of flat-shaped composites were evaluated according to pure water flux and methyl orange model pollution removal performance. Thanks to the homogeneous pore distribution of the composites prepared by the solution precipitation method, the pure water flux of $53 \text{ Lm}^{-2}\text{h}^{-1}\text{bar}^{-1}$ and the MO rejection efficiency were calculated as 46.5% for AgP1. The formation of contamination on the membrane surfaces were analysed and the composite prepared by method I had been found as least rough surface. It was understood that the preparation methods of the composites are the effective variables in porosity, water retention and filtration efficiency.

© 2023 DPU All rights reserved

Keywords: Filtration; polymeric composites; silver particles; contamination accumulation

* Corresponding author. Tel.: +90 228 2142841 E-mail address: hsyngms2016@gmail.com

1. Introduction

Ceramic and polymeric structures are mainly used in the physical separation of pollutants in water. While the high physical and chemical resistance of ceramic structures is the reason for preference. The difficulties in adjusting the pore structure and the high cost have increased the use of polymeric structures. For this reason, synthetic and natural

polymers such as polyvinylidene fluoride (PVDF), polysulfone (PSF), polyether sulfone (PESU), cellulose, cellulose acetate (CA), chitosan and their mixtures are used in filtration applications [1]. The ability to adjust the desired thickness (150-300 μ m) and pore width of the polymer, having good physical and chemical resistance, easy processing and low cost have increased the preference of polymeric composites in filtration applications. This makes it easier to convert PVDF into membranes [2]. Solid or liquid additives added to PVDF in solution form are effective in regulating the pore size and membrane structure. TiO_2/Al_2O_3 doped ultrafiltration PVDF membranes have been used in oil/water separation [3].

Thanks to the increased hydrophilicity, oil separation was achieved and contamination accumulation on the membrane surface was prevented [4]. Polyvinylpyrrolidone was cross-linked to the PVDF surface by grafting method. The sulfobetaine monomers structure formed on the surface pores that acted as sieves [5]. LiCl, clay, and various metal oxides were used as additives to improve the desired properties of the polymer [6], [7]. Ortho phosphoric acid and glycerol added PVDF obtained by the NIPs method in triacetin solution exhibited good CO₂ flux performance thanks to its large pore structure in gas purification [8]. PVDF membrane with dopamine grafted to the surface was activated with silver nanoparticles. The contact angle of membrane gained a high hydrophobic property of 150°.

Cellulosic structures are biodegradable composite materials that can be obtained from various biological materials. Cellulose acetate, carboxymethyl cellulose, methyl cellulose and nano-micro cellulosic structures can be used as membranes directly or by various chemical processes [9]. In addition, cellulose and its derivatives can be prepared from many biomass by various physical and chemical methods and are clean, environmentally friendly alternatives to petroleum-derived composites [10]. Cellulose particles obtained by hydrolyzing textile wastes were dissolved in DMAc and mixed with 50% PVDF to prepare PVDF-Cellulose composites [11]. When the cellulose ratio of the composite reaches 75%, the physical strength decreases. The best composition was obtained at a 1:1 PVDF-Cellulose ratio. Cellulose mixed with PVDF increases the surface hydrophilicity of the structure. In addition, the Ag particles added to the structure provide antimicrobial properties to the composite in addition to the surface properties, and are effective in preventing the accumulation of dirt on the surface of filtration membranes. Due to the wide band gap (3.2 eV), TiO₂ with anatase structure was activated with Ag⁺ to ensure absorption in the visible light region, and the resulting hydrogel was coated on the glass surface by spin coating method. The composite with a surface area of 85-231 m²/g showed 98.86% performance in the catalytic removal of methylene blue and methyl orange from water with photocatalytic effect in the presence of UV [12]. Due to its high UV absorption capacity, TiO2 is frequently used in photocatalytic applications. The addition of silver cation to the structure reduced the energy level between the conduction bands of the molecule and allowed absorption in the visible region.

Silver nano/micro particles are usually made by adding a reductant to the silver salt solution. In addition, many microorganisms, plant extracts and enzymes were used as reductants to obtain Ag particles with the green method [13]. AgNNPs with a size of 32 nm reduced with R. aculeatus plant extract showed high antimicrobial activity against Bacillus subtilis and Enterobacter aerogenes ATCC 13048 [14]. Different reductants, temperatures, mixing rate and times, as well as the method of fixing Ag particles to the composite have the potential to make significant changes in the physical and chemical properties of the composite. In this study, Ag particles were incorporated to PVDF-Cellulose composite mixed with cellulose at a ratio of 1:1 in order to increase the hydrophilic property by two different methods. Ag precipitation with NaBH4 in solution medium (Method I) and PVDF-Cellulose composites with Ag particles added precipitated with NaBH₄ (Method II) were prepared by phase inversion. The physical and filtration performances of membranes incorporating Ag into the PVDF-cellulose polymeric mixture by two different method, precipitation and powder mixing will be examined in this study for the first time according to our literature research. SEM, FTIR and TG-DTA analyses, porosity, water retention and contact angle measurements of the composites were performed. The performance of the composites in removing methyl orange as a model pollutant from water was tested in a filtration cell. Methyl orange is anionic character at neutral pH. It interacts with the membrane surface with the organic groups it contains, making it easier to obtain information about the surface structure. In addition, organic dyes such as methyl orange, Methylene Blue, Congo Red, and Malachite Green are frequently used in industrial activities and cause serious water pollution. Filtration, an advanced version of the traditional adsorption method, is a fast and practical solution.

Due to the functional groups of MO that tend to bond as a result of interaction, their widespread use in industry, and their polluting properties, various methods are being developed to separate them from water. [15,16]. Contamination accumulation of surface experiments and flux performances were reported in this study for Ag incorporated PVDF-Cellulose composites by two different methods.

2. Materials

In our previous study, cellulose particles separated from textile waste were mixed as composite material [11]. Polyvinylidene fluoride (PVDF; Solef 6010, mw:530.000) and analytical grade polymer solvent N,N-Dimethylacetamide (DMAC, 87.12 g/mol, 99%) were purchased from Sigma-Aldrich. Silver nitrate, AgNO₃ (169.87 g/mol, 4.350 g/cm³, ≥99%) and sodium borohydride (37.83 g/mol) were purchased from Sigma-Aldrich as silver salt. Methyl orange (MO, or Orange III) aqueous solution was used as model dye pollutant and distilled water were used as solvent and phase inversion, respectively.

2.1. Preparation of Ag particle added polymeric composites

The synthesis of Ag-doped composites was carried out by two different methods. Method I: 1.6 g of 1:1 PVDF-Cellulose mixture was dissolved in 10 ml of DMAc at 80 °C. Then, AgNO₃ at the amount 10% of the polymer was added in accordance with our former study [13] by stirring in a very small amount of solvent. NaBH₄, equal to the molar ratio of Ag, was added by stirring at a constant temperature. The mixture first turned orange-yellow and then dark brown due to the formation of Ag particles. The solution was poured onto a 20x20 cm glass surface and distributed to a thickness of approximately 250 µm. The glass plate was quickly placed in the water bath and the composite was prepared by phase inversion. The composite containing 10% Ag in proportion to the polymer mass was named AgP1. In the preparation of AgP2 composite with the method II, a polymer solution preparation process similar to AgP1 was applied. For this, first a certain amount of AgNO₃ was dissolved in 100 ml of water. NaBH₄ in Ag molar ratio was added slowly and stirred at 250 rpm. First a yellow then a dark brown precipitate was obtained. The precipitate was filtered and washed with pure water, dried at 40 °C and ground. For the homogenization, ground Ag particles were sieved through a 17-micron sieve. Ag particle at amount 10% of the polymer was added to the solution of PVDF-Cellulose in DMAc and mixed. Then, the mixture spread on the glass was phase inverted in a water bath to obtain AgP2. Ag-free PVDF-cellulose (PC) composite was prepared as a control sample with the same method. Ag particle and composite preparation steps were presented in Fig. 1.

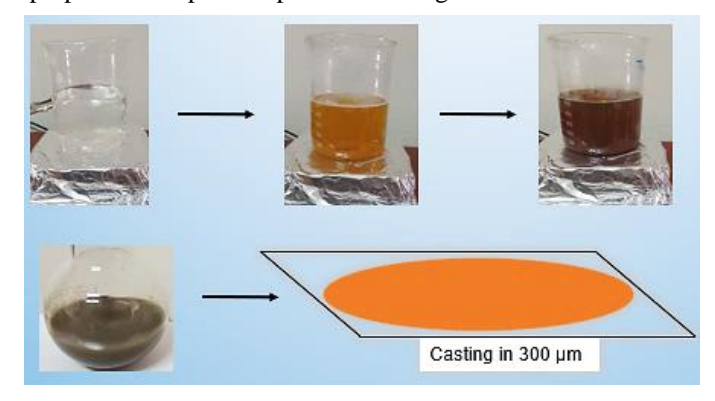


Fig. 1. Illustration of AgP and AgP-doped composite preparation.

2.2. Characterization

The properties of the composites were investigated by functional group, surface images and thermal analysis methods. FTIR analyses were performed with ATR method in the range of 650-4000 cm⁻¹ (Perkin Elmer). For SEM images, gold-coated composite surfaces were scanned at 10 kV power (Carl Size Ultra Plus). For cross-sectional surface images, composites were fractured and imaged in liquid nitrogen. For thermal analyses, 12-15 mg samples were heated at 10 °C/min heating rate in a 5 mL/min nitrogen atmosphere and were performed in the range of 25-700 °C (Seiko Exstar 7200 thermal analyzer). The mass change versus temperature graph was obtained. For the calculation of water retention capacity%, which is an important feature for membranes, the membranes were cut into 2x2 cm dimensions before being wet. They were weighed after being lightly wiped (Ww) by paper, composites were dried at 40 °C for two hours and weighed again (Wd). The same procedures were repeated with 3 repetitions. The WU% capacity of the membranes was calculated according to equation 1:

$$WU(\%) = \frac{W_w - W_d}{W_{w_0}} x 100$$
 (1)

The porosity of the membranes was calculated in terms of %PO according to equation 2;

$$PO(\%) = \frac{W_W - W_d}{dA\delta} \times 100 \tag{2}$$

Here d is the density of pure water (1 g/ml), A is the membrane area (4 cm²) and δ is the thickness value of the wet membrane (cm) determined by the Insize thickness measuring device. Surface hydrophilicity is an indicator of the water permeability of the membranes and is determined by the contact angle measurement. The contact angle values of the membranes were measured with at least 3 repetitions according to the sessile drop method using the KSV Attention, Finland contact angle device.

2.3. Filtration and reusability tests

Pure water flux (PWF) tests of the membranes were performed in a constant flux cell. Flux values were calculated in Lm⁻²h⁻¹bar⁻¹. The flux pressure of the system was tested in the range of 0.5, 1 and 1.5 bar. Pure water was passed through the membranes and conditioned. Pure water flux calculation was made according to equation 3.

$$PWF = \frac{V}{At}$$
 (3)

In this equation, V represents the volume of pure water passing through the membrane (L), A represents the membrane area $(1.7x10^{-3} \text{ m}^2)$, and h represents the flux time. MO removal experiments were performed in the same membrane cell. Previously, the membrane was adjusted to constant flux with pure water. 3L, 40 mg/L MO solution was pumped into the filtration cell. The filtered MO concentration was analyzed in a UV-Vis spectrometer (Shimadzu, 2550) at 466 nm wavelength. MO removal performance was calculated according to equation 4:

$$\mathbf{E}_{\mathbf{AD}}(\%) = \left(\frac{c_0 - c_e}{c_0}\right) \mathbf{x} \mathbf{100} \tag{4}$$

Here C_0 is the initial concentration and C_e is the concentration of the filtered MO solution. The reuse efficiency of the membranes and their resistance to surface contamination were tested. For this purpose, the MO filtered membranes

were washed with 0.25 mol.L^{-1} hydrochloric acid and then the pure water flux values were measured. This process was repeated 3 times. The flux recoveries of the (FRR) membranes were calculated according to equation 5.

$$FRR(\%) = \left(\frac{PWF_3}{PWF_1}\right) \times 100 \tag{5}$$

PWF₁ represents the initial pure water flux of the membrane, PWF₃ represents the flux performance after the 3^{rd} iteration. Using the flux values, the reversible (R_r), irreversible (R_{ir}) and total fouling (R_t) rates resistances against the pollution accumulated on the membrane surface were calculated with equations 6-8 [17].

$$R_r(\%) = \left(1 - \frac{\text{PWF}_3 - \text{PWF}_2}{\text{PWF}_1}\right) \times 100$$
 (6)

$$R_{ir}(\%) = \left(1 - \frac{\text{PWF}_3}{\text{PWF}_1}\right) \times 100 \tag{7}$$

$$R_t(\%) = \left(1 - \frac{PWF_2}{PWF_1}\right) \times 100 \tag{8}$$

3. Results and discussion

3.1. Characterization

Infrared spectrums of pristine and composites presented in Fig.2 indicating the effect of Ag addition by two methods. Although it was mixed with cellulose, the characteristic peaks of PVDF were observed more clearly. This

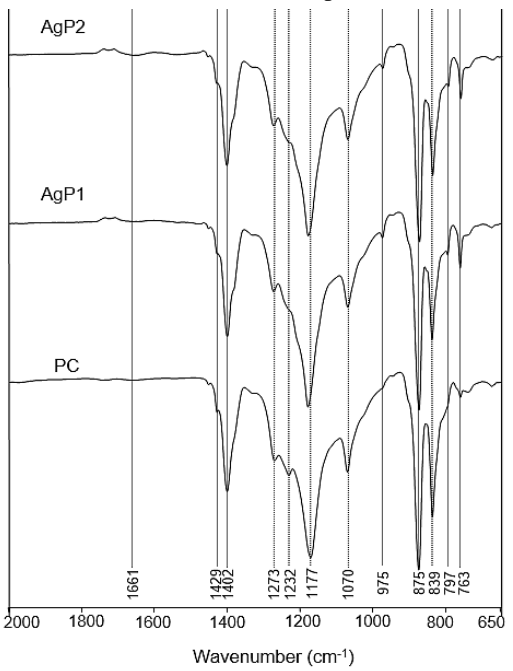


Fig. 2. FT-IR spectrum of PC and composites.

may be due to the differences in structural formation as a result of the PVDF-cellulose-powder interaction. CH and CF₂ bond stretching vibrations for PVDF were observed at 1403 and 877-1175 cm⁻¹ respectively [18]. CF stretching vibration corresponded to at around 1071-1072 cm⁻¹ and no exact change had been observed with Ag addition. α-phases of PVDF in PC could be seen by 763, and 975 cm⁻¹ bands [19]. The bands at around 838-840 cm⁻¹ with 1273 and 1431 cm⁻¹ confirmed the presence of α and β-phases. Intensity of 977 cm⁻¹ increased while a new clear band showing β-PVDF emerged at around 796 cm⁻¹ for all composites [20]. Intensity of characteristic 1232 cm⁻¹ band for PC decreased for modified samples. Reducing intensity of this band and emerging of new bands indicated that Ag addition resulted in noticeable readjustment for crystal phases of polymer and alpha/betha phases of PVDF increased. In addition to changes of crystallinity for PC, the bands emerged at around 1630-1661 cm⁻¹ for AgP1 and AgP2 represents carbonyl groups of amid bending vibrations from primary and secondary amines with the bands at around 1540 cm⁻¹ of N-H vibration [21].

At the SEM images of composites presented in Fig. 3 it was seen that cross section of PC consisted of sponge like (top) and finger-like structures (upper). Finger like channels shrink towards top surface of membrane and turned to pores which are main component for filtration. At the method I, Ag addition to polymer can be seen clearly from the SEM images. Thick skin layer on the top surface of AgP1 was best indicator for changes compared with pristine PC. A well dispersion and interaction of Ag with polymer matrix in dope solution effective due to application method (I). Another important change observed at the top surface of AgP1 was formation of noticeable pores on the surface of membranes. Pores with radius 205-327 nm width formed on the smooth surface of composite membranes. Although AgP2 has similar cross section structure as PC in terms of sponge and finger like structure distribution, tightly sequenced structure of AgP2 can be seen from the images. Agglomerated structures formed on the PC which reduce filtration performances of membrane became more compact. A lot of pores with 182-225 nm width were formed on the top surface of composites. Large quantity of pores indicated that slow phase inversion occurred in the phase inversion process due to high concentration of dope solution. The formation of porous structure on the AgP2 doped PC surface confirmed that phase inversion rate of AgP2 solution was faster than AgP1. It is understood from the results that the preparation method is very important, and that AgP1 creates a nearly uniform surface thanks to

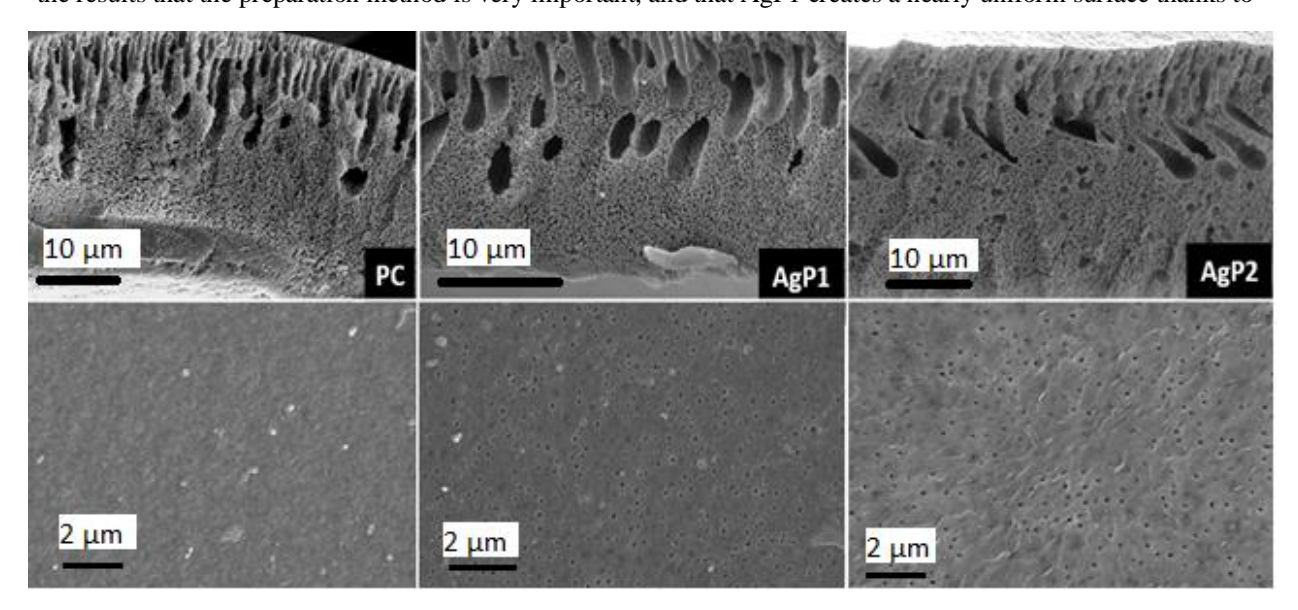


Fig. 3. SEM images of composites, cross section (top) and surface (bottom) respectively.

its homogeneous distribution and controlled nucleation. While precipitation in solution is difficult to control but provides a more homogeneous distribution, powder mixing is easy but results in heterogeneous formations. Thermal decomposition of PC and composites were investigated. Due to organic nature of polymer matrix, and very few amounts of Ag, a little number of residues had been observed after thermal analysis Fig. 4. Decomposition of PC and AgP1, AgP2 occurred at two stages at around 448-470 and 530-542 °C. Decomposition starts with breaking of CH and CF bonds of polymer and progresses by weight loss. Ag addition slightly decreased the decomposition temperature of PC. That may be core effect of Ag that absorb heat. Thus, the thermal degradation of the polymer accelerated. Polymer additives have the potential to alter the thermal behavior of the composite. This change depends on many factors, including the type and amount of additive, the polymer type, and the composite preparation method [22]. Also, dispersion of Ag among polymer chain can make cavities which are called as pores and channels effective in transportation and filtration. These additives weaken the structure rather than clay like additives strengthened effect. At the DTA curves of samples (Fig. 4), main exothermic peak emerged as a result of decomposition of organic structure was observed at decreasing temperatures for all samples. It was recorded at 558 °C for PC however it was 545 and 533 °C for AgP1 and AgP2 respectively. Water uptake and porosity of membranes were measured to observe

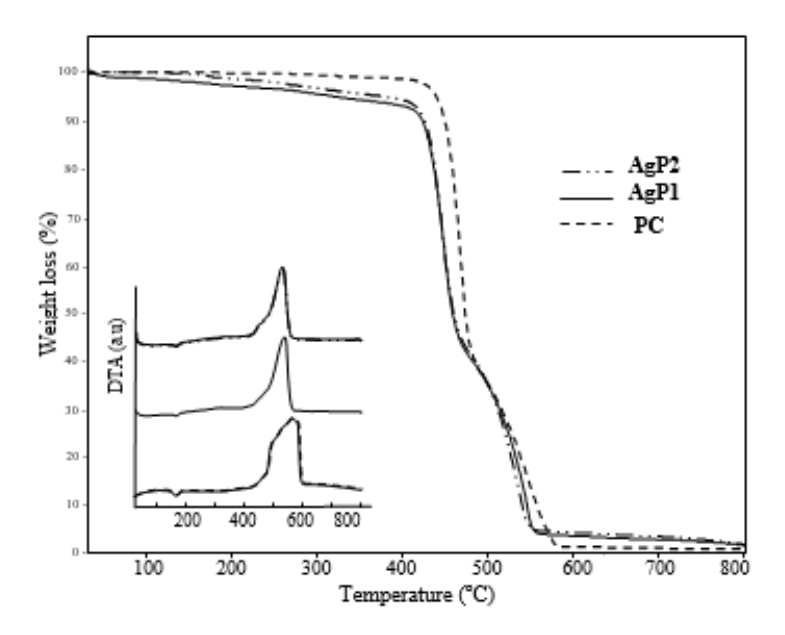


Fig. 3 Thermal analysis curves of PC and composites.

Ag addition effect with different methods. From the results presented at Table 1, water uptake values of AgP1 changed proportionally with its porosity values. Water uptake and porosity of composites were increased to 65.4 and 58.5% respectively. It can be concluded that increase in porosity promoted to increase of water absorbed inside the membrane which consequently measured as increasing at water uptake. Although there is a strong relationship between pore numbers (%) and water absorbed (%) inside the structure of a membrane, a different trend was observed with porosity and water uptake values of AgP2 compared with AgP1. Highest water uptake was obtained with AgP2 membrane. Presumably larger pores were formed inner site of the AgP2 composite due to enlarged molecular structure. The powders added to the polymeric structure is in the form of small particles. So, deviations from homogeneous distribution occurred. As a result, differences in attraction occur in nucleation, which changes the pore size during phase inversion. The surface hydrophilicity of the membranes was investigated. The Ag additive effective in terms of structural change as well as interaction with water molecules in changing the hydrophilicity of the surface. The contact

angle value of the PC composite was recorded as 64° due to the hydrophilic structure of cellulose [23]. The increase in the contact angle of AgP1 indicates that the structure has gained some hydrophobic properties. The reason for this is that the structure has become less rough with the addition of Ag. Thus, the penetration of water molecules into the membrane has slowed down. The reason for this is that the structure has become less rough with the addition of Ag. Thus, the penetration of water molecules into the membrane has slowed down. The main reason for the higher hydrophilicity of AgP2 is its rough surface. The more nonuniform distribution of Ag particles compared to AgP1 has increased the surface roughness. In parallel with this, the penetration of water droplets increased with the wide pores. The contact angle value is an effective parameter in adjusting the surface properties.

Table 1 Properties of composites.

Membrane	Water uptake (%)	Porosity (%)	Contact Angle (°)
PC	56.8±1.1	51.5±1.0	64±1.2
AgP1	65.4 ± 0.7	58.5 ± 0.8	75±1.3
AgP2	69.1 ± 0.8	55.8±1.5	73±1.1

3.2. Filtration results

The filtration tests of the membranes were carried out in a cylindrical flux cell at room temperature in the pressure range of 0.5-1.5 bar. After the permeability of the membrane was incorporated to the appropriate flux value with pure water, the MO solution was filtered. The pure water flux values and MO filtration performance of the membranes are presented in Fig. 5. While the flux values of the Ag-added composites prepared with both methods partially decreased compared to PC, the MO removal values of composites increased. AgP2 exhibited the highest pure water flux and good MO removal. Although the amount of Ag added to the polymer was the same, the change in the membrane structure was different and that affected the flux and removal performance. While the relatively more dispersed and varying-sized pore structure of AgP2 provided high flux performance, it caused a decrease in the MO removal efficiency. The highest MO removal performance of AgP1 was found to be 46.5% (those were 26.2 and 42.9% for PC and AgP2 respectively). The highest MO removal performance of AgP1 can be directly explained by the membrane structure. The solution precipitation method applied in the production of AgP1 provided a more uniform porous membrane thanks to the uniform distribution of Ag particles. The densely arranged and small porous pore structure compared to AgP2 and PC was effective in the removal of MO by AgP1. One of the many parameters affecting the filtration performance is the chemical properties of the filtered material. In this study, the MO solution was tested as a model pollutant at neutral pH value [24]. Heavy metals, medical wastes, organic-inorganic chemicals, dyes-oilspetroleum derivatives are the main substrates separated by filtration [25]. The interaction and bonding of the functional groups of the surface and the substrate or their repulsion is the most important feature that determines the filtration efficiency. Physical or chemical adsorption as a result of the repulsion of opposing groups provides a certain amount of pollution removal from the filtered solution. However, the accumulation of pollutant on the membrane surface usually causes a decrease in flux and therefore a decrease in filtration efficiency [26,27]. The resistance of the membranes to fouling accumulation was analyzed by measuring the pure water flux after MO filtration. After the membranes subjected to MO filtration, they were washed and rinsed in 0.25 mol/L acidic solution for 5 min, the pure water flux performances were measured. The experiments were repeated in 3 replicates and the FRR, reversible (R_r), irreversible (R_{ir}) and total fouling (R_t) values were calculated according to the equation [5-8] and the graphics are given in Fig. 5. When compared with PC, the FRR values of the composites increased, after MO filtration all FRR values decreased with different ratio. The best FRR was obtained with AgP2 with 89.2%. While the large pore structure resulted in decreased MO removal performance, the pores were less blocked. The mechanism of the decrease in the

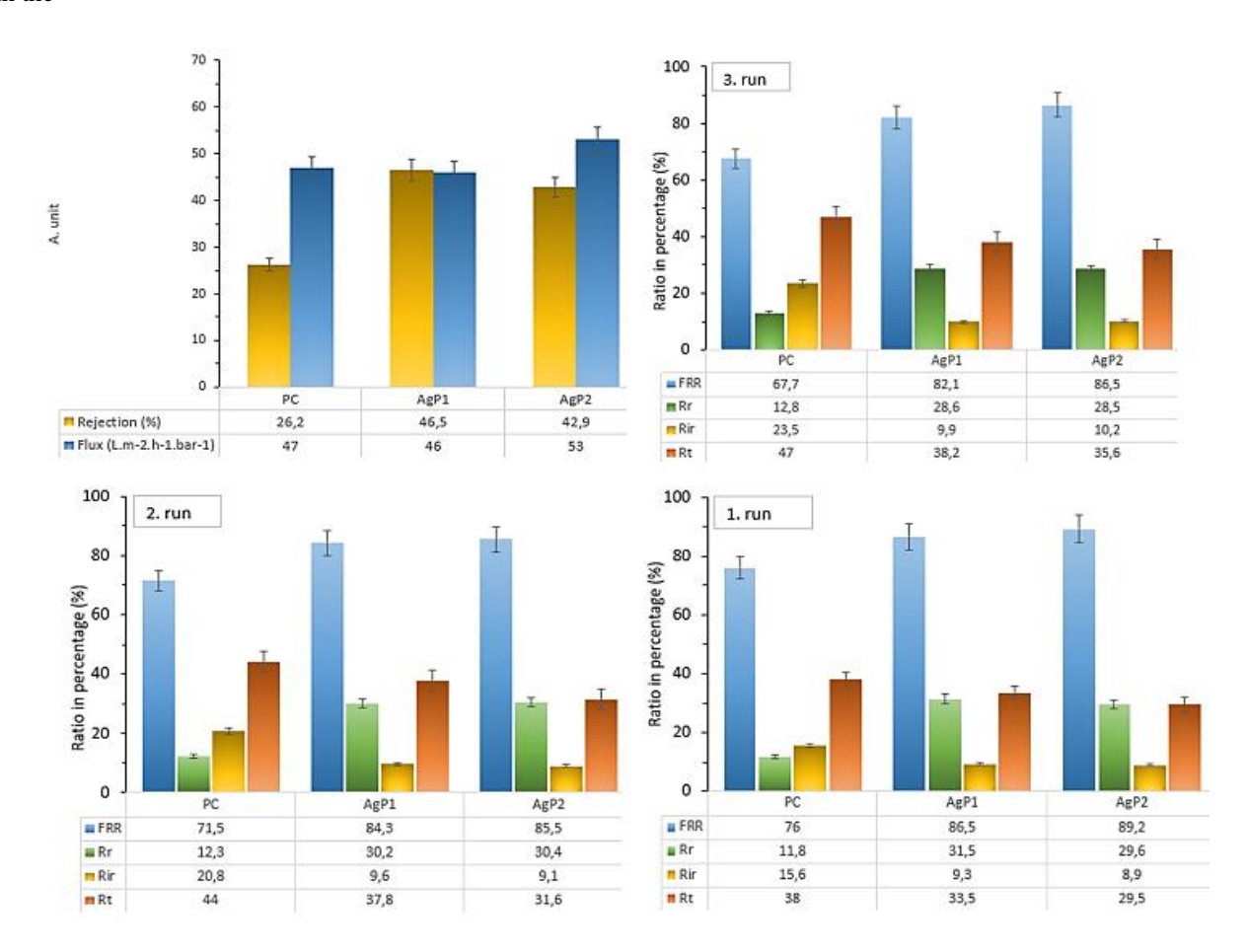


Fig. 5 MO removal and pure water flux, reversible (Rr), irreversible (Rir) and total fouling ratio (Rt) of MO filtrated P and composite membranes during 3-run recycling process. Area: 1.7x10⁻³ m², 1500 mL 40 mg/L MO solution, conditioning pressure = 1 bar, application pressure = 0.5 bar, three consecutive steps of MO filtration (1st step), filtration after water washing (2nd and 3rd step), time of washing = 5 min.

FRR value can be explained by the accumulation of fouling on the membrane surface and in the pores. The change in FRR in repeated uses provides information about the interaction of the fouling with the membrane. The R_r values of PC and composites increased very little rate close to the constant value, whereas R_{ir} reached the highest value only in PC. A little increase was observed in R_{ir} values of composites. These results mean that the MO accumulation on the composite surface occurs with weak interaction. Thus, the removal of contaminants from the surface becomes easier. High Rir indicates that the interaction between the surface and the contaminant molecules may be chemisorption and the clogging is more permanent [28]. R_t , which varies inversely with FRR values, indicates the total fouling value. The highest R_t was calculated with MO filtered PC flux values, while the lowest was obtained with AgP2. Considering the surface properties, AgP2 exhibited better filtration and pollution resistance despite containing roughness suitable for permanent settlement of pollutants. The main reason for this is the pore structure with different dimensions. This difference was effective in continuing its function as a result of clogging of small pores while clogging of large pores

less. There are 8-20% difference among the filtration performance of AgP1 and AgP2. However, the filtration performance of both composites is higher than PC. AgP1 exhibit better efficiency especially in the separation of oil-water mixtures thanks to its high hydrophobic feature. Additive anchoring is a method that has a great effect in regulating many properties of the polymeric structure. AgP1 and AgP2 composites offer different outputs worth applying with their different physical and filtration properties. Hydrophilicity and fouling have complex mechanisms that are shaped by many parameters such as membrane structure, pore volume and number, functional groups of the filtered molecule, and filtration conditions. Therefore, specific evaluation of each composite in terms of the filtered molecule and filtration conditions can yield more accurate results [29].

Conclusions

In this study, the physical and filtration properties of the composites prepared by fixing Ag particles to the PVDF-Cellulose mixture with different methods were investigated. The changes in the functional groups were investigated with FT-IR and the changes in the phase of the polymer were recorded. It was understood from the SEM images that the composites gained different properties as a result of the two methods. While AgP1 prepared with Method I had a more uniform and smoother structure, a rougher and more particle-like structure was formed in AgP2. The Ag additive caused both structures to decompose faster than PC by decreasing the decomposition temperature as a result of thermal heating. Flux, FRR and reusability of membranes were effective in the filtration efficiency. The hydrophobic structure of AgP1, understood from the high contact angle values, was more vulnerable in the accumulation of molecules on the surface. However, the small pores of AgP1 exhibited less resistance to clogging than AgP2. Despite its rough surface suitable for the adhesion of contaminants, AgP2 with heterogeneous pore sizes showed better filtration efficiency. AgP1 exhibited the highest MO removal as 46.5% compared to 26.2% for PC. The type of additive anchoring has the potential to directly affect the structure of the composite, and both Ag-doped composites provided better filtration efficiency than PC.

Acknowledgments

This work was financially supported by TUBİTAK (Scientific and Technological Research Council of Turkey) with grant number 222Z333.

Authors' contributions

Manuscript conception and design, experimental and interpretation, writing and supervision were conducted out by Huseyin Gumus.

References

- [1] Y. Zhang, X. Duan, B. Tan, Y. Jiang, Y. Wang, and T. Qi, "PVDF microfiltration membranes modified with AgNPs/tannic acid for efficient separation of oil and water emulsions," *Colloids and Surfaces A: Physicochemical and Engineering Aspects*, vol. 644, p. 128844, Jul. 2022, doi: 10.1016/j.colsurfa.2022.128844.
- [2] F. Liu, N. A. Hashim, Y. Liu, M. R. M. Abed, and K. Li, "Progress in the production and modification of PVDF membranes," *Journal of Membrane Science*, vol. 375, no. 1, pp. 1–27, Jun. 2011, doi: 10.1016/j.memsci.2011.03.014.
- [3] X. S. Yi *et al.*, "The influence of important factors on ultrafiltration of oil/water emulsion using PVDF membrane modified by nano-sized TiO₂/Al₂O₃," *Desalination*, vol. 281, pp. 179–184, Oct. 2011, doi: 10.1016/j.desal.2011.07.056.
- [4] A. İ. Yucak and F. U. Nigiz, "Emūlsifiye Edilmiş Yağın Polivinilflorür/PolivinilProlidin Membran İle Saflaştırılması," *ejosat*, no. 17, pp. 769–775, doi: 10.31590/ejosat. 643677.
- [5] Q. Li, Q. Bi, H.-H. Lin, L.-X. Bian, and X.-L. Wang, "A novel ultrafiltration (UF) membrane with controllable selectivity for protein separation," *Journal of Membrane Science*, vol. 427, pp. 155–167, Jan. 2013, doi: 10.1016/j.memsci.2012.09.010.
- [6] M. Tomaszewska, "Preparation and properties of flat-sheet membranes from poly(vinylidene fluoride) for membrane distillation," *Desalination*, vol. 104, no. 1, pp. 1–11, Apr. 1996, doi: 10.1016/0011-9164(96)00020-3.

- [7] A. S. Apaydın and P. Onsekizoğlu Bağcı, "Membran Ayırma Tekniklerinin Meyve Suyu İşlemedeki Uygulamaları," *Gıda*, vol. 50, no. 3, pp. 442–465, Jun. 2025, doi: 10.15237/gida.GD25027.
- [8] A. Mansourizadeh, A. F. Ismail, M. S. Abdullah, and B. C. Ng, "Preparation of polyvinylidene fluoride hollow fiber membranes for CO₂ absorption using phase-inversion promoter additives," *Journal of Membrane Science*, vol. 355, no. 1, pp. 200–207, Jun. 2010, doi: 10.1016/j.memsci.2010.03.031.
- [9] Q. Bi, Q. Li, Y. Tian, Y. Lin, and X. Wang, "Hydrophilic modification of poly(vinylidene fluoride) membrane with poly(vinyl pyrrolidone) via a cross-linking reaction," *Journal of Applied Polymer Science*, vol. 127, no. 1, pp. 394–401, 2013, doi: 10.1002/app.37629.
- [10] M. Z. Tufan and C. Özel, "Cellulose and its derivatives as biodegradable materials: A review," *Journal of Scientific Reports-A*, no. 059, pp. 87–104, Dec. 2024, doi: 10.59313/jsr-a.1498226.
- [11] H. Gumus and B. Buyukkidan, "Physicochemical properties and adsorption performances of textile waste based hydrolyzed cellulose-PVDF composites," *Rev. Roum. Chim.*, vol. 67, no. 3, pp. 197–205, 2022, doi: DOI: 10.33224/rrch.2022.67.3.08.
- [12] D. Komaraiah, E. Radha, J. Sivakumar, M. V. Ramana Reddy, and R. Sayanna, "Photoluminescence and photocatalytic activity of spin coated Ag+ doped anatase TiO₂ thin films," *Optical Materials*, vol. 108, p. 110401, Oct. 2020, doi: 10.1016/j.optmat.2020.110401.
- [13] H. Gumus, "Green synthesis of infrared controlled AgNP/graphite/polyvinylidene fluoride composite membranes for removal of organic pollutants," *Journal of Photochemistry and Photobiology A: Chemistry*, vol. 460, p. 116160, Mar. 2025, doi: 10.1016/j.jphotochem.2024.116160.
- [14] F. Karakaya, A. S. Bülbül, M. Bekmezci, and F. Şen, "Silver nanoparticle synthesis by biogenic reduction method and investigation of antimicrobial, antibiofilm, anticancer activities," *Journal of Scientific Reports-A*, no. 055, pp. 1–15, Dec. 2023, doi: 10.59313/jsr-a.1277894.
- [15] L. R. Buddiga, G. R. Gajula, and G. Jaishree, "Methyl Orange Dye degradation of dual doped TiO₂ nanoparticles under visible light Irradiation," *Journal of the Indian Chemical Society*, vol. 102, no. 9, p. 101938, Sep. 2025, doi: 10.1016/j.jics.2025.101938.
- [16] A. Ikhlaq et al., "Catalytic ozonation for the removal of methyl orange in water using iron-coated Moringa oleifera seeds husk," *Process Safety and Environmental Protection*, vol. 199, p. 107248, Jul. 2025, doi: 10.1016/j.psep.2025.107248.
- [17] Z. Chen et al., "Photocatalytic antifouling properties of novel PVDF membranes improved by incorporation of SnO₂-GO nanocomposite for water treatment," Separation and Purification Technology, vol. 259, p. 118184, Mar. 2021, doi: 10.1016/j.seppur.2020.118184.
- [18] Q. Wang, X. Wang, Z. Wang, J. Huang, and Y. Wang, "PVDF membranes with simultaneously enhanced permeability and selectivity by breaking the tradeoff effect via atomic layer deposition of TiO₂," *Journal of Membrane Science*, vol. 442, pp. 57–64, Sep. 2013, doi: 10.1016/j.memsci.2013.04.026.
- [19] F. Shi, Y. Ma, J. Ma, P. Wang, and W. Sun, "Preparation and characterization of PVDF/TiO₂ hybrid membranes with different dosage of nano-TiO₂," *Journal of Membrane Science*, vol. 389, pp. 522–531, Feb. 2012, doi: 10.1016/j.memsci.2011.11.022.
- [20] H. Dzinun, M. H. D. Othman, A. F. Ismail, M. H. Puteh, M. A. Rahman, and J. Jaafar, "Photocatalytic degradation of nonylphenol using co-extruded dual-layer hollow fibre membranes incorporated with a different ratio of TiO₂/PVDF," *Reactive and Functional Polymers*, vol. 99, pp. 80–87, Feb. 2016, doi: 10.1016/j.reactfunctpolym.2015.12.011.
- [21] Y. Mansourpanah and Z. Jafari, "Efficacy of different generations and concentrations of PAMAM–NH₂ on the performance and structure of TFC membranes," *Reactive and Functional Polymers*, vol. 93, pp. 178–189, Aug. 2015, doi: 10.1016/j.reactfunctpolym.2015.04.010.
- [22] A. A. Issa, M. A. Al-Maadeed, A. S. Luyt, D. Ponnamma, and M. K. Hassan, "Physico-Mechanical, Dielectric, and Piezoelectric Properties of PVDF Electrospun Mats Containing Silver Nanoparticles," C, vol. 3, no. 4, Art. no. 4, Dec. 2017, doi: 10.3390/c3040030.
- [23] Y. Ibrahim, E. Abdulkarem, V. Naddeo, F. Banat, and S. W. Hasan, "Synthesis of super hydrophilic cellulose-alpha zirconium phosphate ion exchange membrane via surface coating for the removal of heavy metals from wastewater," *Science of The Total Environment*, vol. 690, pp. 167–180, Nov. 2019, doi: 10.1016/j.scitotenv.2019.07.009.
- [24] H. Gumus and B. Buyukkidan, "Low-cost preparation of photocatalytic hydrolyzed cellulose composites, activated with one-step synthesized graphene oxide-metal oxide for dye degradation," *Cellulose*, vol. 32, no. 7, pp. 4573–4593, May 2025, doi: 10.1007/s10570-025-06521-y.
- [25] S. K. Ramachandran and P. Sathishkumar, "Membrane-based techniques for pollutants removal: An outlook on recent advancements," *Current Opinion in Environmental Science & Health*, vol. 36, p. 100513, Dec. 2023, doi: 10.1016/j.coesh.2023.100513.
- [26] A. Cemanovic, N. Manav, A. Kizilet, and O. Cinar, "Recent advances in membrane fouling control in wastewater treatment processes," vol. 3 no 2, 2019
- [27] Y. A. Tayeh, M. Y. D. Alazaiza, T. M. Alzghoul, and M. J. Bashir, "A comprehensive review of RO membrane fouling: Mechanisms, categories, cleaning methods and pretreatment technologies," *Journal of Hazardous Materials Advances*, vol. 18, p. 100684, May 2025, doi: 10.1016/j.hazadv.2025.100684.
- [28] I. Ounifi et al., "Antifouling Membranes Based on Cellulose Acetate (CA) Blended with Poly(acrylic acid) for Heavy Metal Remediation," Applied Sciences, vol. 11, no. 10, p. 4354, May 2021, doi: 10.3390/app11104354.
- [29] R. Kumar and A. F. Ismail, "Fouling control on microfiltration/ultrafiltration membranes: Effects of morphology, hydrophilicity, and charge," *Journal of Applied Polymer Science*, vol. 132, no. 21, 2015, doi: 10.1002/app.42042.